Charge Separation in a Nonfluorescent Donor−Acceptor Dyad Derived from Boron Dipyrromethene Dye, Leading to Photocurrent Generation

Shigeki Hattori,[†,‡] Kei Ohkubo,[†,‡] Yasuteru Urano,[§] Hisato Sunahara,[§] Tetsuo Nagano,*[,§] Yuji Wada,[†] Nikolai V. Tkachenko,[⊥] Helge Lemmetyinen,*[,⊥] and Shunichi Fukuzumi*[,†,‡]

Department of Material and Life Science, Graduate School of Engineering, Osaka University, Suita, Osaka 565-0871, Japan, SORST, Japan Science and Technology Agency, Suita, Osaka 565-0871, Japan, Graduate School of Pharmaceutical Sciences, The University of Tokyo, Bunkyo-ku, Tokyo 113-0033, Japan, and The Institute of Materials Chemistry, Tampere University of Technology, P.O. Box 541, FIN-33101 Tampere, Finland

Received: February 24, 2005

Boron dipyrromethene (BODIPY), which is commonly used as an energy absorbing and transferring antenna molecule, has been modified to contain an electron donor moiety, 8-(2,4,5-trimethoxyphenyl)-4,4-difluoro-1,3,5,7-tetramethyl-4-bora-3a,4a-diaza-*s*-indacene (**MEOPHBDP**). The photoinduced electron transfer from a 2,4,5-trimethoxyphenyl moiety to a BODIPY moiety of **MEOPHBDP** in acetonitrile was observed by femtosecond laser flash photolysis measurements. The lifetime of the charge-separated state of **MEOPHBDP** was 59 ps at 298 K. The dye-sensitized solar cells (DSSC) were prepared using **MEOPHBDP** with carboxylic acid (**MEOPHBDP−COOH**) and a reference BODIPY dye having no electron donor moiety. The photovoltaic measurements were performed using a standard two-electrode system consisting of a working electrode and a Pt sputtered electrode in methoxyacetonitrile containing 0.5 M iodide and 0.05 M I_2. The photoelectrochemical properties of DSSC with **MEOPHBDP** are compared with those with a reference BODIPY dye.

Introduction

Boron dipyrromethene (BODIPY) fluorophores, which are derived from 4,4-difluoro-1,3,5,7-tetramethyl-4-bora-3a,4a-diaza-*s*-indacene,[1] have been widely employed as useful fluorescence probes for important biomolecules, such as nitric oxide and calcium ion, because a large number of BODIPY derivatives are readily obtained by modification at carbon positions at 1, 3, 5, 7, and 8.[2−4] The fluorescence imaging is the most powerful technique currently available for continuous observation of the dynamic intracellular events of living cells.[5−7] The attractive characteristics of BODIPY derivatives include sharp (fwhm ∼ 25 nm) and moderately strong absorption near 500 nm (ϵ = 40 000−100 000 M^{-1} cm^{-1}), large quantum yields, long excited-state lifetimes (ca. 5 ns for boron-dipyrrin dyes),[4] good solubility in organic solvents, and amenability toward chromatography on silica and alumina.[8−10] These characteristics are compatible with the photochemical properties of a zinc porphyrin.[11−13] Extensive efforts have therefore been devoted to design and synthesize zinc porphyrin-linked BODIPY dyads, in which BODIPY is used as an energy absorbing and transferring antenna and zinc porphyrin acts as an energy acceptor from the antenna moiety.[8−10,14] Such dyads have been extended to develop a system capable of absorbing light, transferring the excitation energy to an energy acceptor, and using the excitation energy to start photoinduced electron transfer, followed by subsequent multielectron-transfer steps, leading to a long-range charge separation as a mimic of the photosynthetic reaction center.[15,16] However, BODIPY itself has never been used to start photoinduced electron transfer.

We report herein that a BODIPY derivative, 8-(2,4,5-trimethoxyphenyl)-4,4-difluoro-1,3,5,7-tetramethyl-4-bora-3a,4a-diaza-*s*-indacene (**MEOPHBDP**),[17] in which an electron donor moiety (2,4,5-trimethoxyphenyl group) is directly linked at the 8 position of the BODIPY moiety, undergoes efficient charge separation upon photoexcitation of the BODIPY moiety. The occurrence of the charge separation is directly monitored by the femtosecond laser flash photolysis measurements. The resulting BODIPY radical anion has the ability to inject an electron into the conduction band of TiO_2 as indicated by photocurrent generation in a dye-sensitized solar cell (DSSC)[18,19] using **MEOPHBDP** with carboxylic acid, 8-(2,4,5-trimethoxyphenyl)-2,6-dicarboxyethyl-4,4-difluoro-1,3,5,7-tetramethyl-4-bora-3a,4a-diaza-*s*-indacene (**MEOPHBDP−COOH**), which is adsorbed on TiO_2. The photoelectrochemical properties of a donor−acceptor-type DSSC with **MEOPHBDP−COOH** and a DSSC with the corresponding reference compound without an electron donor moiety, 8-phenyl-2,6-dicarboxyethyl-4,4-difluoro-1,3,5,7-tetramethyl-4-bora-3a,4a-diaza-*s*-indacene (**PHBDP−COOH**). The BODIPY derivatives used in this study are shown in Figure 1.

Experimental Section

Materials. The preparation of **MEOPHBDP**, **MEOPHBDP−COOH**, and **PHBDP−COOH** has been described elsewhere.[17] Tetra-*n*-butylammonium perchlorate (TBAP), used as a supporting electrolyte for the electrochemical measurements, was obtained from Tokyo Kasei Kogyo Co., Ltd., recrystallized from ethanol, and dried in vacuo prior to use. All solvents, LiI, 1,2-dimethyl-3-propylimidazolium iodide, *tert*-butylpyridine, and methoxyacetonitrile, were of reagent grade quality, purchased and used without further purification unless otherwise noted.

* Corresponding author. E-mail: fukuzumi@chem.eng.osaka-u.ac.jp.
† Osaka University.
‡ SORST, Japan Science and Technology Agency.
§ The University of Tokyo.
⊥ Tampere University of Technology.

10.1021/jp050952x CCC: $30.25
Published on Web 07/23/2005

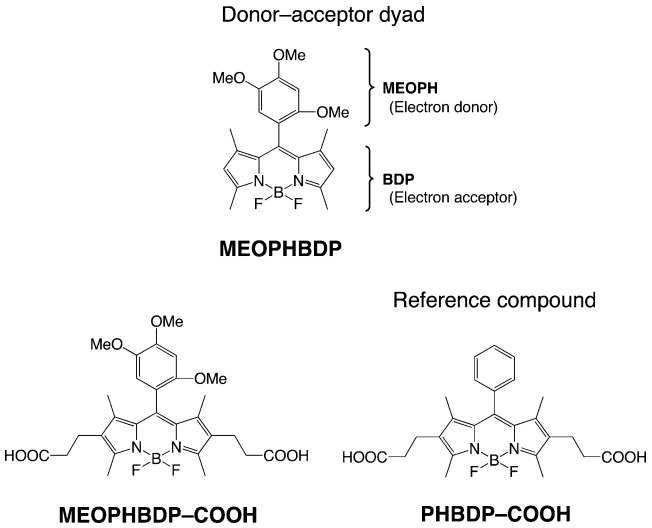

Figure 1. Structures of compounds used in this study.

Electrochemical Measurement. Cyclic voltammetry measurements were performed on an ALS 630 A electrochemical analyzer using a three-electrode arrangement in a single cell with a Pt wire counter electrode, a Pt disk working electrode, and an $Ag/AgNO_3$ (0.01 M) reference electrode (BAS). The sample solutions contained a BODIPY derivative (1.0×10^{-3} M) and 0.1 M TBAP as a supporting electrolyte in acetonitrile (MeCN). Determined potentials (vs Ag/Ag^+) were converted to those vs SCE by adding 0.29 V.[21] UV−vis. spectroelectrochemical experiments were performed with a thin-layer spectroelectrochemical quartz cell (path-length of 0.5 mm) using a three-electrode arrangement: light transparent platinum gauze (100 mesh, 0.07 mm diameter) as an working electrode, a platinum wire counter electrode, and an $Ag/AgNO_3$ (0.01 M) reference electrode. Potentials were applied with a HOKUTO DENKO HSV-100 electrochemical analyzer. The electrochemical reaction was monitored with a Shimadzu UV-3100 spectrophotometer. All electrochemical measurements were carried out under an atmospheric pressure of argon.

Time-Resolved Absorption Measurements. Femto- to picosecond time-resolved absorption spectra were collected using a pump−probe technique as described elsewhere.[22] The femtosecond pulses of the Ti:sapphire generator were amplified by using a multipass amplifier (CDP-Avesta, Moscow, Russia) pumped by a second harmonic of the Nd:YAG Q-switched laser (model LF114, Solar TII, Minsk, Belorussia). The amplified pulses were used to generate a second harmonic (420 nm) for sample excitation (pump beam) and white continuum for a time-resolved spectrum detection (probe beam). The samples were placed into 1 mm rotating cuvettes, and averaging of 100 pulsed at a 10 Hz repetition rate was used to improve the signal-to-noise ratio. The typical response time of the instrument was 150 fs (fwhm). A global multiexponential fitting procedure was applied to process the data. The procedure takes into account the instrument time response function and the group velocity dispersion of the white continuum and allowed calculation of the decay time constants and dispersion−compensated transient absorption spectra. Nanosecond transient absorption measurements were carried out using a Nd:YAG laser (Solar, TII) at 355 nm as an excitation source. The solution was deoxygenated by argon purging for 15 min prior to measurements.

Fluorescence Lifetime Measurements. Ultrafast fluorescence decays were measured by an up-conversion method as described previously.[23] The instrument (FOG100, CDP, Moscow, Russia) utilizes the a second harmonic (420 nm) of a 50 fs pulsed Ti:sapphire laser (TiF50, CDP, Moscow, Russia) pumped by an Ar ion laser (Innova 316P, Coherent). The samples were placed into a rotating disk-shaped 1 mm cuvette. A typical time resolution for the instrument was 150 fs (fwhm).

Theoretical Calculations. Density-functional theory (DFT) calculations were performed on a COMPAQ DS20E computer. Geometry optimizations were carried out using the Becke3LYP functional and 6-31G* basis set,[24,25] with the restricted Hartree−Fock (RHF) formalism and as implemented in the Gaussian 98 program.[26] A graphical output of the computational results was generated with the Cerius[2] software program developed by Molecular Simulations Inc.

Preparation of Dye-Sensitized Solar Cells. Nanoporous TiO_2 electrodes were prepared by dropping the colloidal suspensions of TiO_2 nanoparticles (P25, $d = 21$ nm, Nippon Aerogel) on an optically transparent electrode (OTE) (Nippon Sheet Glass, SnO_2:F, 8 Ω/square) with a glass rod and adhesive tapes as a spacer. The resulting electrodes (OTE/TiO_2) were annealed at 450 °C in air for 30 min. The thickness of the electrodes ranged between 13 and 14 μm as measured by a profiler.

Nanoporous $ZnO-SnO_2$ electrodes were prepared by the following procedure.[27,28] A colloidal 15% aqueous dispersion of SnO_2 (Alpha Chemicals) of crystallite size ∼0.015 μm (3.0 mL), acetic acid (0.1 mL), and ZnO of crystallite size ∼0.5 μm (0.6 g) were ground in an agate mortar, mixed with 7 mL of a methanol−water (1:1) mixture, and agitated for 10 min. The dispersion was then sprayed onto OTE ($OTE/ZnO-SnO_2$), and the resulting electrodes were annealed at 450 °C in air for 30 min. The thickness of the electrodes ranged between 13 and 14 μm as measured by a profiler.

The coloration of the oxide semiconductor surface with **MEOPHBDP−COOH** was carried out by immersing the film (still warm, i.e., 80−100 °C) for 12 h in a *tert*-butyl alcohol−MeCN (1:1) mixture containing 3.0×10^{-4} M of the dye. After the completion of the dye adsorption, the electrode was withdrawn from the solution, washed with MeCN, and dried. After the **MEOPHBDP−COOH**-coated film was immersed in 0.1 M NaOH (aq) solution overnight, the dye was desorbed from the film into solution, which was used to determine the amount of dye molecules adsorbed onto the film by measuring the absorbance. The numbers of dye molecules adsorbed on oxide semiconductors (molecules cm^{-2}) were calculated from measurement areas (cm^2). The UV−visible spectra were recorded on a Shimadzu UV-3100PC spectrophotometer. Fluorescence measurements of BODIPY derivatives were performed on a Shimadzu RF-5300PC spectrofluorophotometer.

Photoelectrochemical Measurements. Photocurrent−voltage characteristics of solar cells were measured using a voltage−current source monitor (Advantest R6246) under an AM1.5 simulated light source (Yamashita Denso, YSS-80). Incident photon-to-photocurrent efficiency (IPCE) measurements were performed using a setup for IPCE measurement (PV-25DYE, JASCO) under 5 mW cm^{-2} monochromatic light illuminations. Solar cells were made by placing a Pt sputtered optically transparent electrode (F-doped SnO_2 sheet resistance 10 Ω/square, Asahi Glass) on the dye-coated semiconductor film, and then the electrolyte was introduced from the edge of the two glass substrates just before the measurements.

Results and Discussion

Redox and Photophysical Properties. A cyclic voltammogram of **MEOPHBDP** in MeCN containing 0.1 M TBAP is illustrated in Figure 2. A reversible one-electron reduction is

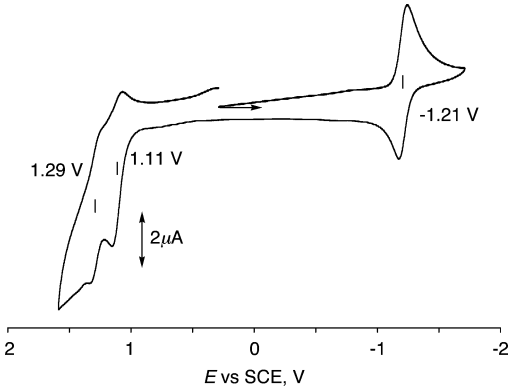

Figure 2. The cyclic voltammogram of **MEOPHBDP** (3.5×10^{-4} M) in deoxygenated MeCN containing 0.1 M TBAP; sweep rate = 0.1 V s^{-1}.

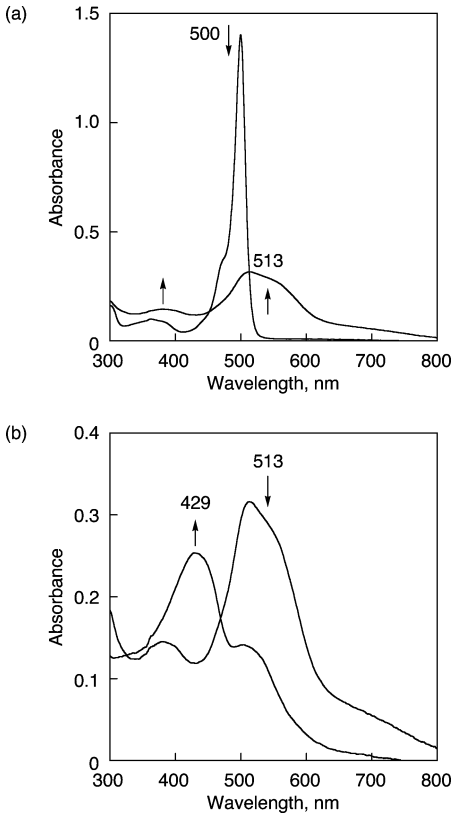

Figure 3. Thin-layer UV−visible spectra before and after (a) first oxidation with applied potential at 1.24 V vs SCE and (b) second oxidation with applied potential at 1.49 V vs SCE of **MEOPHBDP** (3.5×10^{-4} M) in deoxygenated MeCN containing TBAP (0.1 M).

observed for the BODIPY moiety, whereas two reversible one-electron oxidations are seen for both the MEOPH and BODIPY moieties. To assign the site of oxidation, the UV−visible spectra upon the electrochemical oxidation of **MEOPHBDP** were measured using a thin-layer cell as shown in Figure 3. The UV−visible spectra are seen for the first oxidation product of **MEOPHBDP** (λ_{max} = 380 and 515 nm) and the second oxidation of **MEOPHBDP** (λ_{max} = 430 nm). The absorption

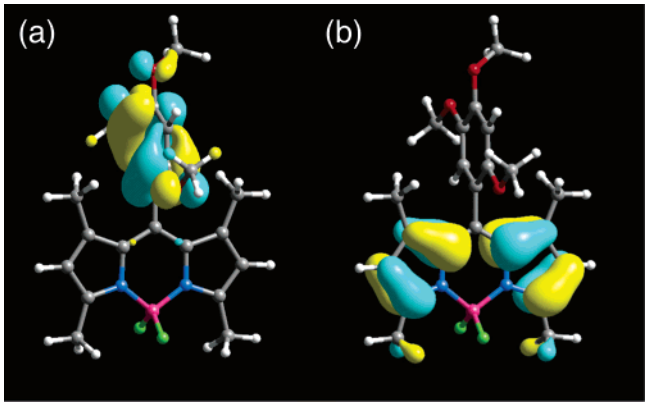

Figure 4. (a) HOMO-1 and (b) LUMO orbitals of **MEOPHBDP**. The geometry optimization was calculated by a DFT method with Gaussian 98 (B3LYP/6-31G* basis set).

spectrum of the second oxidation of **MEOPHBDP** is characteristic of that of a 2,4,5-trimethoxybenzene moiety radical cation.[29] Thus, the two reversible one-electron oxidations observed in Figure 2 are assigned to the one-electron oxidation of the BODIPY moiety (1.11 V vs SCE) and the one-electron oxidation of the 2,4,5-trimethoxybenzene moiety (1.29 V vs SCE), respectively. The one-electron redox potentials of the BODIPY derivatives, which were determined by the cyclic voltammetry measurements, are listed in Table 1. The one-electron oxidation and reduction potentials of the BODIPY moiety in **MEOPHBDP−COOH** (1.05 V and −1.35 V vs SCE) are nearly the same as those of the BODIPY moiety in **PHBDP−COOH** (1.02 V and −1.34 V vs SCE). The one-electron oxidation potential of the MEOPH moiety in **MEOPHBDP−COOH** (1.27 V vs SCE) is also virtually the same as that of the MEOPH moiety in **MEOPHBDP** (1.29 V vs SCE).

The absorption and emission spectra of **MEOPHBDP**, **MEOPHBDP−COOH**, and **PHBDP−COOH** were measured in MeCN and the resulting data are also listed in Table 1.

The fluorescence of **MEOPHBDP** is significantly quenched by electron transfer from the 2,4,5-trimethoxybenzene (MEOPH) moiety to the singlet excited state of the BODIPY moiety (BDP) of **MEOPHBDP**. The fluorescence quantum yields of **MEOPHBDP** are determined as 0.0001, which is significantly smaller than those of the typical BODIPY dyes due to the fluorescence quenching by the photoinduced electron transfer in **MEOPHBDP**. According to the DFT calculations (see the Experimental Section), the HOMO-1 and LUMO orbitals of **MEOPHBDP** are localized on the MEOPH moiety and BDP moiety, respectively, as shown in Figure 4.

Figure 5 shows the fluorescence decay curve at 511 nm of **MEOPHBDP** in deoxygenated MeCN excited at 420 nm. The first-order fit gives the value of the lifetime (τ) of 1.2 ps for this component as shown in Figure 5, which is much shorter as compared to the usual BODIPY without an electron donor moiety dye (e.g., τ_0 = 3.2 ns of 8-phenyl-4,4-difluoro-1,3,5,7-tetramethyl-4-bora-3a,4a-diaza-*s*-indacene, **PHBDP**).[30] Such a short fluorescence lifetime of **MEOPHBDP** results from electron transfer from the donor moiety (MEOPH) to the singlet

TABLE 1: Absorption and Emission Maxima and One-Electron Oxidation (E_{ox}) and Reduction (E_{red}) Potentials of MEOPHBDP, MEOPHBDP−COOH, and PHBDP−COOH in Dearerated MeCN

compd	abs λ_{max}, nm	em λ_{max}, nm	E_{ox} (vs SCE), V MEOPH$^{\bullet+}$/MEOPH	E_{ox} (vs SCE), V BDP$^{\bullet+}$/BDP	E_{red} (vs SCE), V BDP/BDP$^{\bullet-}$
MEOPHBDP	500	511	1.29	1.11	−1.21
MEOPHBDP−COOH	524	537	1.27	1.05	−1.35
PHBDPCOOH	520	534		1.02	−1.34

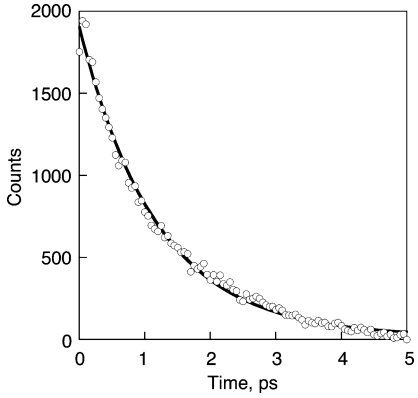

Figure 5. Fluorescence decay curve of **MEOPHBDP** (1.0×10^{-5} M) in deoxygenated MeCN; the excitation wavelength = 420 nm.

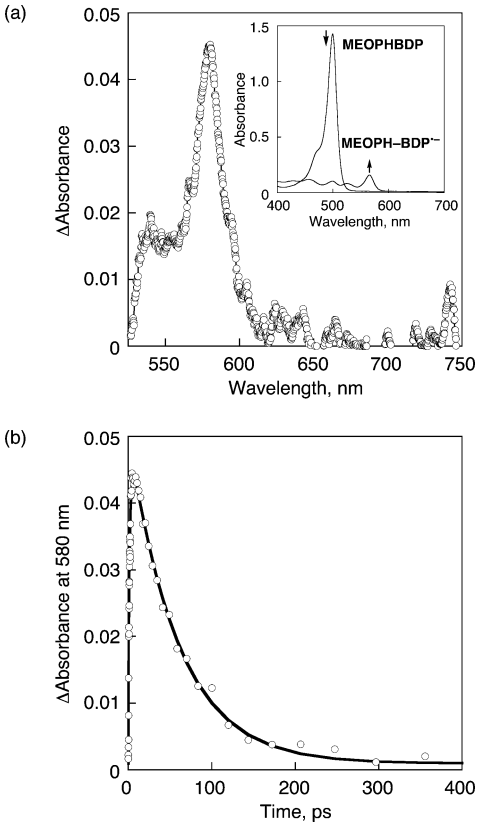

Figure 6. (a) Transient absorption spectra of **MEOPHBDP** (1.0×10^{-5} M) in deoxygenated MeCN at 298 K taken at 3.5 ps after laser pulse excitation at 420 nm. The inset shows the thin-layer UV−visible spectra before and after electrochemical reduction with applied potential at −1.31 vs SCE of **MEOPHBDP** (3.5×10^{-4} M) in deoxygenated MeCN containing TBAP (0.1 M). (b) Decay profile at 580 nm observed in the photoreaction of **MEOPHBDP** after laser excitation at 420 nm.

excited state of the acceptor moiety, BODIPY (BDP), as confirmed by the transient absorption spectrum (vide infra). The electron-transfer rate constant (k_{et}) is calculated from the fluorescence lifetime of **MEOPHBDP** (τ) in reference to that of the reference compound (τ_0) by eq 1 as 8.5×10^{11} s^{-1}.

$$k_{et} = \tau_f^{-1} - \tau_0^{-1} \quad (1)$$

A deaerated MeCN solution containing **MEOPHBDP** gives rise, upon a 420 nm femtosecond laser pulse, to a transient absorption spectrum with maximum at 580 nm, as shown in Figure 6A. The absorption band at 580 nm is ascribed to the BODIPY radical anion ($BDP^{\bullet-}$), since the one-electron reduction of BODIPY in a thin-layer cell yields the radical anion of BODIPY, which exhibits the same absorption band at about 580 nm (Figure 6A inset). On the other hand, the absorption band of 2,4,5-trimethoxybenzene moiety radical cation ($MEOPH^{\bullet+}$) is not observed under the present experimental conditions, because the absorption band of $MEOPH^{\bullet+}$ appears at around 300, 410, and 450 nm,[29] which is out of our measurement range. The decay of absorbance at 580 nm obeyed first-order kinetics with the rate constant of 1.7×10^{10} s^{-1}, as shown in Figure 6B.

The first-order decay kinetics correspond to the back-electron transfer from the $BDP^{\bullet-}$ to the $MEOPH^{\bullet+}$ moiety in the radical ion pair to regenerate the original ground state. This result indicates that the single excited state of the BODIPY moiety in **MEOPHBDP** is quenched to form the short-lived charge-separated state with a lifetime of 59 ps at 298 K.

Absorption Properties of TiO_2 Electrodes Modified with MEOPHBDP−COOH and PHBDP−COOH. BODIPY dyes with carboxylic acid, **MEOPHBDP−COOH** and **PHBDP−COOH**, are adsorbed on the oxide semiconductor surface by immersing the film in a *tert*-butyl alcohol−MeCN (1:1) mixture containing the dye, respectively (see Experimental Section). The absorption spectra of dyes in solution and TiO_2 films modified with the dyes are shown in Figure 7. The λ_{max} values of the dyes in solution are 524 nm for **MEOPHBDP−COOH** and 520 nm for **PHBDP−COOH**, whereas the absorption spectra of the dyes adsorbed on the TiO_2 surface are obviously broadened as compared with those in H_2O. Such broadening indicates that the molecular environment on OTE/TiO_2 is significantly perturbed because of the aggregation of the dye molecules.

The dyes were desorbed with 0.1 M NaOH (aq) solutions. The numbers of dye molecules adsorbed on TiO_2 films are determined from the absorbance of desorbed dyes in solution using the molar absorption coefficients (ϵ) at the wavelength of maximum absorbance (λ_{max}) of dyes (69 000 M^{-1} cm^{-1} for **MEOPHBDP−COOH** and 74 000 M^{-1} cm^{-1} for **PHBDP−COOH**). The numbers of **MEOPHBDP−COOH** and **PHBDP−COOH** adsorbed on TiO_2 films were determined as 1.6×10^{16} and 1.5×10^{16} molecules cm^{-2}, respectively. The numbers of adsorbed dye molecules of **MEOPHBDP−COOH** and **PHBDP−COOH** are approximately the same.

Photoelectrochemical Properties of MEOPHBDP−COOH and PHBDP−COOH Derivatives on OTE/TiO_2. To evaluate the response of BODIPY derivatives toward the photocurrent generation, a series of photocurrent action spectra were recorded. The monochromatic incident photon-to-photocurrent conversion efficiency (IPCE), defined as the number of electrons generated by light in the outer circuit divided by the number of incident photons, was determined by using eq 2,[31]

$$\text{IPCE}\ (\%) = 100 \times 1240 \times I_{sc}(\text{mA cm}^{-2})/[\lambda(\text{nm}) \times P_{in}(\text{mW cm}^{-2})] \quad (2)$$

where I_{sc} is the short circuit photocurrent generated by monochromatic light and λ is the wavelength of incident monochromatic light, and whose light intensity is P_{in}.

Figure 8A shows the photocurrent action spectra of **MEOPHBDP−COOH** and **PHBDP−COOH** on the OTE/TiO_2 electrode. The maximum IPCE values of OTE/TiO_2/**MEOPHBDP−COOH** and OTE/TiO_2/**PHBDP−COOH** electrodes are 2.0% and 3.1% in the visible region, respectively. The results are summarized in Table 2. Although the IPCE values of OTE/TiO_2/**MEOPHBDP−COOH** are lower than those of OTE/TiO_2/

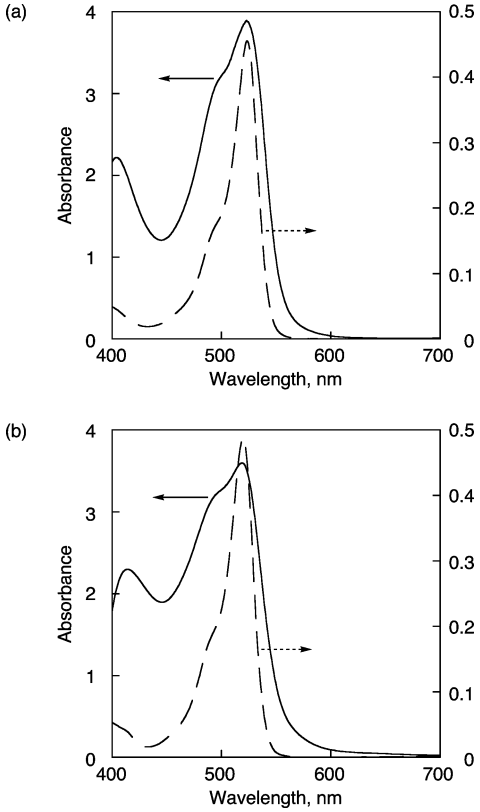

Figure 7. (a) Absorption spectra of OTE/TiO_2/**MEOPHBDP**−**COOH** electrode (solid line) and **MEOPHBDP**−**COOH** (6.5×10^{-6} M) in H_2O (dashed line). (b) Absorption spectra of OTE/TiO_2/**PHBDP**−**COOH** electrode (solid line) and **PHBDP**−**COOH** (6.5×10^{-6} M) in H_2O (dashed line).

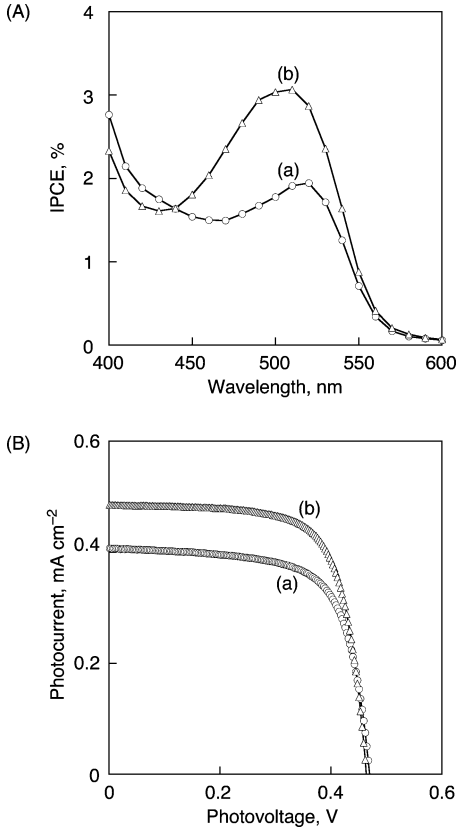

Figure 8. (A) Comparison of photocurrent action spectra (IPCE values) of (a) OTE/TiO_2/**MEOPHBDP**−**COOH** with (b) OTE/TiO_2/**PHBDP**−**COOH** electrodes. (B) Photocurrent−photovoltage curves of (a) OTE/TiO_2/**MEOPHBDP**−**COOH** and (b) OTE/TiO_2/**PHBDP**−**COOH** electrodes under white light illumination. Electrolyte: 0.5 M LiI, 0.05 M I_2, 0.3 M 1,2-dimethyl-3-propylimidazolium iodide, and 0.5 M *tert*-butylpyridine in methoxyacetonitrile. Input power = 100 mW cm^{-2}.

PHBDP−**COOH**, it should be noted that appreciable photocurrent generation is observed for OTE/TiO_2/**MEOPHBDP**−**COOH** in which the dye is virtually nonfluorescent due to the efficient electron transfer from the donor moiety, 2,4,5-trimethoxybenzene (MEOPH), to the singlet excited state of the acceptor moiety, BODIPY (BDP), as confirmed by the transient absorption spectrum (vide supra).

The current−voltage ($I-V$) characteristics of BODIPY derivatives on OTE/TiO_2 were examined using a thin-layer sandwich-type solar cell under illumination of simulated AM 1.5 solar light (100 mW cm^{-2} from a Xe lamp) to determine the light energy conversion efficiency (η). The dye-coated TiO_2 film as working electrode was placed directly on top of an OTE as a counter electrode, on which Pt was sputtered. The redox electrolyte was introduced into the interelectrode space by capillary force. The solar cells were illuminated in the front through a conducting glass substrate. Light energy conversion efficiency (η) is calculated by eq 3,[32]

$$\eta = \mathrm{FF} \times I_{sc} \times V_{oc}/P_{in} \quad (3)$$

where the fill factor (FF) is defined as $\mathrm{FF} = [IV]_{max}/I_{sc}V_{oc}$, where V_{oc} is the open-circuit photovoltage and I_{sc} is the short circuit photocurrent.

Figure 8B shows the $I-V$ characteristics of **MEOPHBDP**−**COOH** and **PHBDP**−**COOH** on OTE/TiO_2. The short circuit photocurrents (I_{sc}), open-circuit photovoltages (V_{oc}), and fill factors (FF) are summarized in Table 2 together with the light energy conversion efficiencies (η), which are determined with eq 3. The η values are 0.13% for an OTE/TiO_2/**MEOPHBDP**−**COOH** electrode and 0.16% for an OTE/TiO_2/**PHBDP**−**COOH** electrode.

TABLE 2: Performance Characteristics of OTE/TiO_2/MEOPHBDP−COOH and OTE/TiO_2/PHBDP−COOH Electrodes under White Light Illumination[a]

	MEOPHBDP−COOH	**PHBDP−COOH**
I_{sc}, mA cm^{-2}	0.41	0.49
V_{oc}, mV	470	464
FF	0.68	0.71
η, %	0.13	0.16
IPCE, % (λ, nm)	2.0 (520)	3.1 (510)

[a] Electrolyte: 0.5 M LiI, 0.05 M I_2, 0.3 M 1,2-dimethyl-3-propylimidazolium iodide, and 0.5 M *tert*-butylpyridine in methoxyacetonitrile. Input power = 100 mW cm^{-2}.

The relatively lower photovoltaic properties of BODIPY-sensitized solar cells might be due to the aggregation of dyes on the TiO_2 surface. To prevent the aggregation for dyes on the TiO_2 surface, the adsorbed amount of BODIPY dyes was reduced by the adsorption of cholic acid derivatives[33] together with BODIPY dyes on the TiO_2 electrode. The cholic acid derivatives have been previously reported in the case of black dye[34] and coumarin dyes[35] to obtain higher photovoltaic properties. The dye solutions were prepared in a *tert*-butyl alcohol−MeCN (1:1) mixture of (1.5×10^{-4} M), to which 1.5×10^{-4} M chenodeoxycholic acid (CCA) was added. The TiO_2 electrodes modified with both BODIPY dye and CCA were similarly prepared (OTE/TiO_2/**MEOPHBDP**−**COOH**+CCA and OTE/TiO_2/**PHBDP**−**COOH**+CCA). The absorbance of OTE/TiO_2/**MEOPHBDP**−**COOH**+CCA and OTE/TiO_2/**PHBDP**−**COOH**+CCA electrodes become lower than those of the corresponding single-component electrodes (OTE/TiO_2/

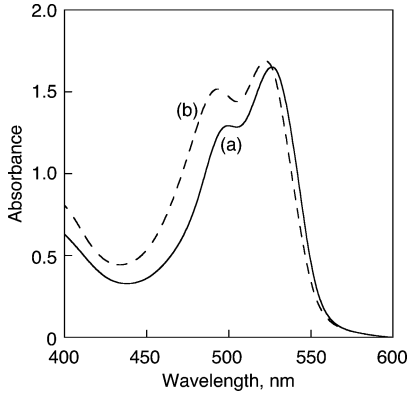

Figure 9. Absorption spectra of (a) OTE/ZnO−SnO_2/**MEOPHBDP−COOH** and (b) OTE/ZnO−SnO_2/**PHBDP−COOH** electrodes.

MEOPHBDP−COOH and OTE/TiO_2/**PHBDP−COOH**), respectively (see the Supporting Information, S1). The numbers of **MEOPHBDP−COOH** and **PHBDP−COOH** adsorbed on these electrodes were determined as 9.2×10^{15} and 8.7×10^{15} molecules cm^{-2}, respectively. The adsorbed amount of **MEOPHBDP−COOH** and **PHBDP−COOH** was approximately one-half as compared to the case of corresponding single-component electrodes. The photovoltaic measurements using OTE/TiO_2/**MEOPHBDP−COOH**+CCA and OTE/TiO_2/**PHBDP−COOH**+CCA were performed. No improvement of the photovoltaic properties of OTE/TiO_2/**MEOPHBDP−COOH**+CCA and OTE/TiO_2/**PHBDP−COOH**+CCA was observed as compared with the case of the corresponding single-component electrodes (see the Supporting Information, S2 and S3). Thus, the relatively lower photovoltaic properties of the DSSCs may not be ascribed to the aggregation of dyes on the TiO_2 surface.

Light Energy Conversion Properties of MEOPHBDP−COOH and PHBDP− COOH Derivatives on ZnO−SnO_2 Composite Films. Tennakone et al. have reported that DSSCs assembled on ZnO−SnO_2 composite nanoparticles (OTE/ZnO−SnO_2) exhibit more efficient light energy conversion as compared with the corresponding DSSCs on TiO_2 nanoparticles.[27,28] Thus, we also examined DSSCs of BODIPY derivatives assembled on ZnO−SnO_2 composite nanoparticles in comparison with those on TiO_2. The DSSCs on ZnO−SnO_2 composite nanoparticles were made by a similar method employed for the preparation of OTE/TiO_2 films.[27,28] The numbers of adsorbed dye molecules of **MEOPHBDP−COOH** and **PHBDP−COOH** on ZnO−SnO_2 films (1.4×10^{17} molecules cm^{-2} for **MEOPHBDP−COOH**, 1.5×10^{17} molecules cm^{-2} for **PHBDP−COOH**) are significantly larger than those of OTE/TiO_2 films. The absorption spectra of ZnO−SnO_2 films sensitized with dyes are shown in Figure 9 (the film thickness of the electrodes for UV−vis measurements ranged between 2 and 3 μm as measured by a profiler, because ZnO−SnO_2 films scatter irradiated light). The absorption spectrum of **MEOPHBDP−COOH** and **PHBDP−COOH** adsorbed on the ZnO−SnO_2 surface is obviously broadened as in the case of earlier dye-sensitized TiO_2 systems.

The photocurrent generation is also observed in both cases of OTE/ZnO−SnO_2/**MEOPHBDP−COOH** and OTE/ZnO−SnO_2/**PHBDP−COOH** electrodes. Figure 10 shows the photocurrent action spectra of OTE/ZnO−SnO_2/**MEOPHBDP−COOH** and OTE/ZnO−SnO_2/**PHBDP−COOH** electrodes. The IPCE values of **MEOPHBDP−COOH** and **PHBDP−COOH** on the OTE/ZnO−SnO_2 electrodes in Figure 10A are similar to those of the corresponding OTE/TiO_2 electrodes in Figure 8A.

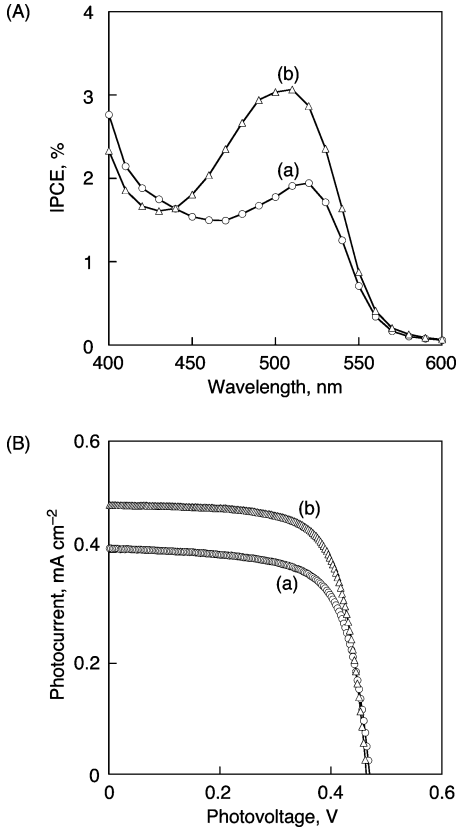

Figure 10. (A) Comparison of photocurrent action spectra (IPCE values) of (a) OTE/ZnO−SnO_2/**MEOPHBDP−COOH** and (b) OTE/ZnO−SnO_2/**PHBDP−COOH** electrodes. (B) Photocurrent−photovoltage curves of (a) OTE/ZnO−SnO_2/**MEOPHBDP−COOH** and (b) OTE/ZnO−SnO_2/**PHBDP−COOH** electrodes under white light illumination. Electrolyte: 0.5 M LiI, 0.05 M I_2, 0.3 M 1,2-dimethyl-3-propylimidazolium iodide, and 0.5 M *tert*-butylpyridine in methoxyacetonitrile. Input power = 100 mW cm^{-2}.

TABLE 3: Performance Characteristics of OTE/ZnO−SnO_2/MEOPHBDP−COOH and OTE/ZnO−SnO_2/PHBDP−COOH Electrodes under White Light Illumination

	MEOPHBDP−COOH	PHBDP−COOH
I_{sc}, mA cm^{-1}	0.29	0.38
V_{oc}, mV	430	430
FF	0.43	0.42
η, %	0.54	0.070
IPCE, % (λ, nm)	2.1 (520)	2.9 (510)

[a] Electrolyte: 0.5 M LiI, 0.05 M I_2, 0.3 M 1,2-dimethyl-3-propylimidazolium iodide, and 0.5 M *tert*-butylpyridine in methoxyacetonitrile. Input power = 100 mW cm^{-2}.

The $I-V$ characteristics of **MEOPHBDP−COOH** and **PHBDP−COOH** on the OTE/ZnO−SnO_2 electrodes are shown in Figure 10B. The resulting data are listed in Table 3. The η values in Table 3 are lower than those in Table 1 because of low FF value. Despite the large number of dye molecules that cover the surface of the ZnO−SnO_2 composite film as compared with those on the TiO_2 film, the suppression of the electron exchange between the dye-covered ZnO−SnO_2 film and redox couple (I_3^-/I^-) may result in the decrease in the FF values.

Mechanism of Photocurrent Generation. The photocurrent generation in the organic dye-sensitized solar cells (DSSC) has previously been reported to be initiated by ultrafast electron injection from the singlet excited state of the dye into the conduction band of the semiconductor in the femtosecond time domain.[36,37] In the case of the reference compounds (**PHBDP−COOH**), the photoexcitation of the BODIPY (BDP) moiety

results in electron injection from the singlet excited state of the dye ($BDP^{\bullet+}/BDP^{*} = -1.11$ V vs NHE)[38] into the TiO_2 conduction band (−0.5 V vs NHE) and/or trap states to produce the BODIPY radical cation ($BDP^{\bullet+}$), since no electron donor moiety is linked with the BODIPY moiety in **PHBDP−COOH**. The resulting BODIPY radical cation ($BDP^{\bullet+}/BDP = 1.3$ V vs NHE) produced in the photoinduced electron injection to the conduction band of TiO_2 is reduced by electrolyte ($I_3^-/I^- =$ 0.5 V vs NHE).[19,39] At the counter electrode, the electron reduces the oxidized electrolyte, I_3^-, leading to photocurrent generation.

In the case of **MEOPHBDP−COOH**, the photoexcitation of the BODIPY moiety results in photoinduced electron transfer from the MEOPH moiety to the singlet excited state of the BODIPY (BDP) moiety.[40] The resulting $BDP^{\bullet-}$ can inject an electron to the conduction band of the semiconductor,[41] because the redox potential of $BDP/BDP^{\bullet-}$ (−1.11 V vs NHE) is lower than that of the conduction band (−0.5 V vs NHE).[19] On the other hand, $MEOPH^{\bullet+}$ is reduced by I^- ($E(I_3^-/I^-) = 0.5$ V vs NHE) to regenerate MEOPH. The electron is collected at the back contact to perform electrical work in the external circuit. At the counter electrode, the electron reduces electrolyte, I_3^-.

Conclusions

The photoinduced electron transfer occurs from the 2,4,5-trimethoxybenzene (MEOPH) moiety to the singlet excited state of the BODIPY (4,4-difluoro-1,3,5,7-tetramethyl-4-bora-3a,4a-diaza-*s*-indacene) moiety (BDP) in a simple donor−acceptor dyad (**MEOPHBDP**) derived from BODIPY to afford the charge-separated state ($MEOPH^{\bullet+}-BDP^{\bullet-}$). The charge separation rate is very fast (8.5×10^{11} s^{-1}), and the back-electron-transfer rate (1.7×10^{10} s^{-1}) is slower than the charge separation rate. This enabled us to detect the charge-separated state ($MEOPH^{\bullet+}-BDP^{\bullet-}$) by femtosecond laser flash photolysis measurements. The charge-separated state has been shown to have the ability to inject an electron to the conduction band of TiO_2 of the **MEOPHBDP−COOH**-sensitized solar cell despite the absence of fluorescence, leading to the photocurrent generation. In the case of the solar cell based on fluorescent **PHBDP−COOH**, the photoexcitation of the BODIPY moiety results in direct electron injection from the singlet excited state of the dye, leading to the photocurrent generation.

Acknowledgment. This work was partially supported by a Grant-in-Aid (No. 16205020) from the Ministry of Education, Culture, Sports, Science, and Technology, Japan, and by the Academy of Finland and the National Technology Agency in Finland. We are grateful to Dr. Takayuki Kitamura, Osaka University, for helping preparation of DSSC.

Supporting Information Available: Absorption spectra of OTE/TiO_2/**MEOPHBDP−COOH**+CCA and OTE/TiO_2/**PHBDP−COOH**+CCA electrodes (S1), IPCE values and *I*−*V* curves of OTE/TiO_2/**MEOPHBDP−COOH**+CCA and OTE/TiO_2/**PHBDP−COOH**+CCA electrodes (S2), and performance characteristics of OTE/TiO_2/**MEOPHBDP−COOH**+CCA and OTE/TiO_2/**PHBDP−COOH**+CCA electrodes (S3). This material is available free of charge via the Internet at http://pubs.acs.org.

References and Notes

(1) Treibs, A.; Kreuzer, F. H. *Liebigs Ann. Chem*. **1968**, *718*, 208.

(2) Wories, H. J.; Koek, J. H.; Lodder, G.; Lugtenburg, J.; Fokkens, R.; Driessen, O.; Mohn, G. R. *Recl. Trav. Chim. Pays-Bas* **1985**, *104*, 288.

(3) Haugland, R. P. *Handbook of Fluorescent Probes and Research Chemicals*, 6th ed; Molecular Probes: Eugene, OR, 1996.

(4) Karolin, J.; Johansson, L. B.-A.; Strandberg, L.; Ny, T. *J. Am. Chem. Soc.* **1994**, *116*, 7801.

(5) (a) de Silva, A. P.; Gunaratne, H. Q. N.; Gunnlaugsson, T.; Huxley, A. J. M.; McCoy, C. P.; Rademacher, J. T.; Rice, T. E. *Chem. Rev.* **1997**, *97*, 1515. (b) Bissell, R. A.; de Silva, A. P.; Gunaratne, H. Q. N.; Lynch, P. L. M.; Maguire, G. E. M.; Sandanayake, K. R. A. S. *Chem. Soc. Rev.* **1992**, *21*, 187.

(6) (a) Minta, A.; Kao, J. P. Y.; Tsien, R. Y. *J. Biol. Chem.* **1989**, *264*, 8171. (b) Zalewski, P. D.; Forbes, I. J.; Betts, W. H. *Biochem. J.* **1993**, *296*, 403.

(7) *Biophysical and Biochemical Aspects of Fluorescence Spectroscopy*; Dewey, T. G., Ed.; Plenum: New York, 1991.

(8) Van Patten, P. G.; Shreve, A. P.; Lindsey, J. S.; Donohoe, R. J. *J. Phys. Chem. B* **1998**, *102*, 4209.

(9) (a) Li, F.; Yang, S. I.; Ciringh, Y.; Seth, J.; Martin, C. H., III; Singh, D. L.; Kim, D.; Birge, R. R.; Bocian, D. F.; Holten, D.; Lindsey, J. S. *J. Am. Chem. Soc.* **1998**, *120*, 10001. (b) Lammi, R. K.; Wagner, R. W.; Ambroise, A.; Diers, J. R.; Bocian, D. F.; Holten, D.; Lindsey, J. S. *J. Phys. Chem. B* **2001**, *105*, 5341.

(10) (a) Wagner, R. W.; Lindsey, J. S. *J. Am. Chem. Soc*. **1994**, *116*, 9759. (b) Wagner, R. W.; Lindsey, J. S.; Seth, J.; Palaniappan, V.; Bocian, D. F. *J. Am. Chem. Soc.* **1996**, *118*, 3996. (c) Wagner, R. W.; Lindsey, J. S. *Pure Appl. Chem*. **1996**, *68*, 1373.

(11) (a) Gust, D.; Moore, T. A. In *The Porphyrin Handbook*; Kadish, K. M., Smith, K. M., Guilard, R., Eds.; Academic Press: San Diego, CA, 2000; Vol. 8, pp 153−190. (b) Gust, D.; Moore, T. A.; Moore, A. L. *Acc. Chem. Res.* **2001**, *34*, 40.

(12) (a) Wasielewski, M. R. *Chem. Rev.* **1992**, *92*, 435. (b) Osuka, A.; Mataga, N.; Okada, T. *Pure Appl. Chem*. **1997**, *69*, 797.

(13) Fukuzumi, S.; Guldi, D. M. In *Electron Transfer in Chemistry*; Balzani, V., Ed.; Wiley-VCH: Weinheim, Germany, 2001; Vol. 2, pp 270−337.

(14) Kumaresan, D.; Datta, A.; Ravikanth, M. *Chem. Phys. Lett.* **2004**, *395*, 87.

(15) Imahori, H.; Norieda, H.; Yamada, H.; Nishimura, Y.; Yamazaki, I.; Sakata, Y.; Fukuzumi, S. *J. Am. Chem. Soc*. **2001**, *123*, 100.

(16) D'Souza, F.; Smith, P. M.; Zandler, M. E.; McCarty, A. L.; Itou, M.; Araki, Y.; Ito, O. *J. Am. Chem. Soc.* **2004**, *126*, 7898.

(17) **MEOPHBDP** was developed as one of the BODIPY fluorescence sensors; see: Gabe, Y.; Urano, Y.; Kikuchi, K.; Kojima, H.; Nagano, T. *J. Am. Chem. Soc.* **2004**, *126*, 3357.

(18) (a) O'Regan, B.; Grätzel, M. *Nature* **1991**, *353*, 737. (b) Hagfeldt, A.; Grätzel, M. *Chem. Rev.* **1995**, *95*, 49. (c) Hagfeldt, A.; Grätzel, M. *Acc. Chem. Res.* **2000**, *33*, 269.

(19) Grätzel, M.; Moser, J. E. In *Electron Transfer in Chemistry*; Balzani, V., Ed.; Wiley-VCH: Weinheim, Germany, 2001; Vol. 5; pp 589−644.

(20) Fukuzumi, S.; Yorisue, Y. *Bull. Chem. Soc. Jpn*. **1992**, *65*, 715.

(21) Mann, C. K.; Barnes, K. K. *Electrochemical Reactions in Nonaqueous Systems*; Marcel Dekker: New York, 1970.

(22) Tkachenko, N. V.; Rantala, L.; Tauber, A. Y.; Helaja, J.; Hynninen, P. H.; Lemmetyinen, H. *J. Am.* Chem. Soc. **1999**, *121*, 9378.

(23) Tkachenko, N. V.; Grandell, D.; Ikonen, M.; Jutila, A.; Moritz, V.; Lemmetyinen, H. *Photochem. Photobiol*. **1993**, *58*, 284.

(24) (a) Becke, A. D. *J. Chem. Phys.* **1993**, *98*, 5648. (b) Lee, C.; Yang, W.; Parr, R. G. *Phys. Rev. B* **1988**, *37*, 785.

(25) Hehre, W. J.; Radom, L.; Schleyer, P. v. R.; Pople, J. A. *Ab Initio Molecular Orbital Theory*; Wiley: New York, 1986.

(26) Frisch, M. J.; Trucks, G. W.; Schlegel, H. B.; Scuseria, G. E.; Robb, M. A.; Cheeseman, J. R.; Zakrzewski, V. G.; Montgomery, J. A., Jr.; Stratmann, R. E.; Burant, J. C.; Dapprich, S.; Millam, J. M.; Daniels, A. D.; Kudin, K. N.; Strain, M. C.; Farkas, O.; Tomasi, J.; Barone, V.; Cossi, M.; Cammi, R.; Mennucci, B.; Pomelli, C.; Adamo, C.; Clifford, S.; Ochterski, J.; Petersson, G. A.; Ayala, P. Y.; Cui, Q.; Morokuma, K.; Malick, D. K.; Rabuck, A. D.; Raghavachari, K.; Foresman, J. B.; Cioslowski, J.; Ortiz, J. V.; Stefanov, B. B.; Liu, G.; Liashenko, A.; Piskorz, P.; Komaromi, I.; Gomperts, R.; Martin, R. L.; Fox, D. J.; Keith, T.; Al-Laham, M. A.; Peng, C. Y.; Nanayakkara, A.; Gonzalez, C.; Challacombe, M.; Gill, P. M. W.; Johnson, B. G.; Chen, W.; Wong, M. W.; Andres, J. L.; Head-Gordon, M.; Replogle, E. S.; Pople, J. A. *Gaussian 98*, revision A.7; Gaussian, Inc.: Pittsburgh, PA, 1998.

(27) (a) Tennakone, K.; Kumara, G. R. R. A.; Kottegoda, I. R. M.; Perera, V. P. S. *Chem. Commun.* **1999**, 15. (b) Tennakone, K.; Kottegoda, I. R. M.; De Silva, L. A. A.; Perera, V. P. S. *Semicond. Sci. Technol.* **1999**, *14*, 975.

(28) Kumara, G. R. A.; Konno, A.; Tennakone, K. *Chem. Lett.* **2001**, 180.

(29) O'Neill, P.; Steenken, S.; Schulte-Frohlinde, D. *J. Phys. Chem.* **1975**, *79*, 2773.

(30) Kollmannnsberger, M.; Rurack, K.; Resch-Genger, U.; Daub, J. *J. Phys. Chem. A* **1998**, *102*, 10211.

(31) Khazraji, A. C.; Hotchandani, S.; Das, S.; Kamat P. V. *J. Phys. Chem. B* **1999**, *103*, 4693.

(32) (a) Kamat, P. V.; Barazzouk, S.; Thomas, K. G.; Hotchandani, S. *J. Phys. Chem. B* **2000**, *104*, 4014. (b) Sudeep P. K.; Ipe, B. I.; Thomas, K. G.; George, M. V.; Barazzouk, S.; Hotchandani, S.; Kamat, P. V. *Nano Lett.* **2002**, *2*, 29. (c) Kamat, P. V.; Barazzouk, S.; Hotchandani, S.; Thomas, K. G. *Chem. Eur. J.* **2000**, *6*, 3914.

(33) Kay, A.; Grätzel, M. *J. Phys. Chem.* **1993**, *97*, 6272.

(34) Nazeeruddin, M. K.; Péchy, P.; Renouard, T.; Zakkeruddin, S. M.; Humphry-Baker, R.; Comte, P.; Liska, P.; Cevey, L.; Costa, E.; Shklover, V.; Spiccia, L.; Deacon, G. B.; Bignozzi, C. A.; Grätzel, M. *J. Am. Chem. Soc.* **2001**, *123*, 1613.

(35) Hara, K.; Kurashige, M.; Dan-oh, Y.; Kasada, C.; Shinpo, A.; Suga, S.; Sayama, K.; Arakawa, H. *New J. Chem.* **2003**, *27*, 783.

(36) Benkö, G.; Skårman, B.; Wallenberg, R.; Hagfeldt, A.; Sundström, V.; Yartsev, A. P. *J. Phys. Chem. B* **2003**, *107*, 1370.

(37) Pelet, S.; Grätzel, M.; Moser, J.-E. *J. Phys. Chem. B* **2003**, *107*, 3215.

(38) The redox potential (vs SCE) is converted to that vs NHE by adding 0.24 V; see ref 21.

(39) (a) Hasobe, T.; Imahori, H.; Fukuzumi, S.; Kamat, P. V. *J. Mater. Chem.* **2003**, *13*, 2515. (b) Hasobe, T. Imahori, H.; Fukuzumi, S.; Kamat, P. V. *J. Phys. Chem. B* **2003**, *107*, 12105.

(40) The oxidation potential (E^0_{ox}) of the MEOPH moiety (MEOPH$^{\bullet+}$/MEOPH) and the reduction potential (E^0_{red}) of the BDP moiety (BDP/BDP$^{\bullet-}$) in **MEOPH−COOH** are determined as 1.27 vs SCE and −1.35 vs SCE, respectively. The singlet excitation energy (ΔE) is determined as 2.34 eV from the wavelength of absorption and fluorescence maxima. The free energy change of electron transfer from the MEOPH moiety to the singlet excited state of the BDP moiety to produce the radical ion pair (ΔG_{et}) is given by $\Delta G_{et} = e(E^0_{ox} - E^0_{red}) - \Delta E + w_p$, in which e is elementary charge and w_p is the electrostatic interaction energy in the radical ion pair (MEOPH$^{\bullet+}$ and BDP$^{\bullet-}$). The occurrence of photoinduced electron transfer in Figure 6a indicates that the w_p value is more negative than 0.28 eV. With regard to the w_p term of the electron donor−acceptor dyad, see: Miura, T.; Urano, Y.; Tanaka, K.; Nagano, T.; Ohkubo, K.; Fukuzumi, S. *J. Am. Chem. Soc.* **2003**, *125*, 8666.

(41) A similar mechanism involving charge separation in the dye has been reported previously; see: (a) Hattori, S.; Hasobe, T.; Ohkubo, K.; Urano, Y.; Umezawa, N.; Nagano, T.; Wada, Y.; Yanagida, S.; Fukuzumi, S. *J. Phys. Chem. B* **2004**, *108*, 15200. (b) Hasobe, T.; Hattori, S.; Kotani, H.; Ohkubo, K.; Hosomizu, K.; Imahori, H.; Kamat, P. V.; Fukuzumi, S. *Org. Lett.* **2004**, *6*, 3103.